Heliyon 9 (2023) e20649

Contents lists available at ScienceDirect

Heliyon

journal homepage: www.cell.com/heliyon

CircUSP10 promotes liver cancer progression by regulating miR-211-5p/TCF12/EMT signaling pathway

Xiang Chen [a,b,1], Yao Xu [b,1], Zhengyang Zhou [c], Ping Zhao [b], Zhou Zhou [d], Feng Wang [d], Fengyun Zhong [c,**], Hong Du [a,*]

[a] Department of Clinical Laboratory, The Second Affiliated Hospital of Soochow University, Suzhou 215004, China
[b] Department of Laboratory Medicine, Nantong First People's Hospital and The Second Affiliated Hospital of Nantong University, Medical School of Nantong University, Nantong 226001, China
[c] Department of General Surgery, The Second Affiliated Hospital of Soochow University, Suzhou 215004, China
[d] Department of Laboratory Medicine, Affiliated Hospital of Nantong University, Medical School of Nantong University, Nantong 226001, China

ARTICLE INFO

Keywords:
circUSP10
miR-211-5p
TCF12
LC
EMT

ABSTRACT

There is no precise diagnosis or prognosis for liver cancer (LC) using a single biomarker. Circular RNAs (circRNAs) contribute to the pathogenesis of different cancers, but their role in LC is not entirely understood. In this study, circUSP10, an aberrantly expressed circRNA in LC, was screened using the Gene Expression Omnibus database, and its tissue-specific expression was verified using qRT-PCR. In vitro, functional assays and nude mouse tumorigenesis models were used to investigate circUSP10 role in LC. RNA immunoprecipitation and dual-luciferase reporter assays were performed to study the mechanistic relationship between circUSP10, miR-211-5p, and transcription factor 12 (TCF12). We found that circUSP10 expression was upregulated in LC tissues and cells. CircUSP10 expression was linked to tumor size and tumor node metastasis stage and negatively correlated with LC prognosis. In vitro assays confirmed circUSP10-mediated proliferation, migration, and invasion of LC cells and their association with the epithelial-mesenchymal transition (EMT) pathway. Mechanistically, circUSP10 adsorbed miR-211-5p, which regulated TCF12 and promoted tumorigenesis via the EMT signaling pathway. Therefore, our results suggest that circUSP10 may promote LC progression by modulating the miR-211-5p/TCF12/EMT signaling cascade and may serve as a potential biomarker for LC diagnosis and prognosis.

1. Introduction

Primary liver cancer (LC) is the sixth most common cancer and the third leading cause of cancer-related deaths worldwide [1]. Since most LC is insidious and progresses promptly, the onset of symptoms is generally at an advanced stage [2,3]. Alpha-fetoprotein (AFP) is a well-known and extensively used clinical diagnostic biomarker for primary LC [4]. However, its diagnostic value is limited to primary LC, and not all patients with LC are diagnosed at an early stage using AFP [5]. The lack of early diagnosis has led to

* Corresponding author. Department of Clinical Laboratory, The Second Affiliated Hospital of Soochow University, Suzhou 215004, China.
** Corresponding author
E-mail addresses: zfysz@126.com (F. Zhong), hong_du@126.com (H. Du).
[1] Xiang Chen and Yao Xu contributed equally to this work.

https://doi.org/10.1016/j.heliyon.2023.e20649
Received 15 May 2023; Received in revised form 22 September 2023; Accepted 3 October 2023
Available online 4 October 2023

unsatisfactory treatment of LC. Therefore, it is imperative to identify new biomarkers that may assist in the clinical diagnosis, treatment, and prognosis of LC.

In contrast to linear mRNAs, circRNAs belong to a class of non-coding RNAs formed by reverse cyclization of the 5′ and 3′ ends after splicing the precursor mRNA (pre-mRNA) [6]. CircRNAs exist stably in cells and tissues, have a long half-life, and resist RNase R cleavage. These properties may be related to their ring structure, which lacks the 5′ cap structure and 3′ poly(A) tail of mRNAs [7]. Most circRNAs are composed of exons, are evolutionarily conserved, and may be expressed explicitly in a given tissue. Their expression abundance is linked to the developmental stage or age [8,9]. Studies have demonstrated multiple biological functions of circRNAs. For example, circRNAs may act as sponges for miRNAs, regulate subsequent target genes, serve as templates for protein translation, or act in combination with regulatory proteins [10–12]. circRNAs are closely associated with cancer development and may participate in tumor proliferation, metastasis, and apoptosis [13,14]. A fraction of aberrantly expressed circRNAs have been shown to participate in LC pathogenesis. For instance, circ-G004213 in LC may regulate sensitivity to cisplatin by acting as an miR-513b-5p sponge, consequently affecting PRPF39 [15]. In addition, circβ-catenin was also found to encode a protein segment that activates Wnt/β-catenin signaling and promotes LC growth [16]. However, the relationship between circRNAs and LC remains unclear and warrants further investigation.

Epithelial-mesenchymal transition (EMT) refers to the reduction in adhesion between epithelial cells and the enhancement of movement, which transforms into mesenchymal characteristics [17]. EMT is an important link between cell and cancer development [18]. EMT plays a role in the progression of liver, gastric, lung, breast, and colorectal cancers and influences tumor metastasis and invasiveness [19]. The high expression of FoxP4 in hepatocellular carcinoma affects the mRNA and protein expression of E-cadherin and N-cadherin. It promotes cell proliferation, migration, and invasion by regulating the EMT-related molecule Slug [20]. LncRNA RP11-619L19.2 is upregulated in colon cancer (CC) tissues and cell lines and can affect CC progression by regulating miR-1271-5p/CD164/EMT, which is helpful for clinical diagnosis and treatment [21].

This study screened a novel circRNA, hsa_circRNA_101889 (circUSP10), upregulated in LC. We confirmed that circUSP10 affected TCF12 by adsorbing miR-211-5p, ultimately influencing LC progression via the EMT pathway. Therefore, we hypothesized that circUSP10 is a potential biomarker for LC diagnosis and could serve as a novel therapeutic target.

2. Methods and materials

2.1. Clinical sample collection

Sixty-seven paired LC and para-cancerous tissue specimens were collected between April 2019 and April 2020 from the Affiliated Hospital of Nantong University and the Nantong Third People's Hospital. None of the patients with the selected tissues underwent prior radiotherapy or chemotherapy. Clinical samples were collected from patients after informed consent was obtained. This study was approved by the Ethics Committee of the Affiliated Hospital of Nantong University (approval number:2019-L071), and all regulations were met. After resection, tissue samples were snap-frozen frozen (liquid nitrogen) for further experiments.

2.2. Cell culture

LC cells (SK-Hep-1, BEL-7404, SMMC-7721, MHCC-97H, and HCCLM3) and a normal liver cell line (LO2) were obtained from Cell Bank/Stem Cell Bank, Chinese Academy of Sciences. A complete medium (with 5 mL of fetal bovine serum in 45 mL of basal medium plus 0.5 mL of triple antibody) was used for cell culture. LO2 and LC cell lines were cultivated in RPMI-1640 medium (Corning, NY, USA) and DMEM (Corning) in a humidified atmosphere of 37 °C and 5 % CO_2. The medium was replenished or changed depending on the cell growth.

2.3. Total RNA extraction, reverse transcription reactions, and qRT-PCR

An appropriate amount of cells or ground tissue was added to 1 mL of TRIzol Reagent (Thermo Fisher Scientific, Waltham, MA, USA), shaken, mixed, and then placed on ice for 15 min for lysis. The samples were treated with chloroform, isopropanol, and 75 % ethanol to extract the total RNA. After quantification, the RNA was reverse-transcribed according to the instructions of the reverse transcription kit (Thermo Fisher Scientific), and subjected to qRT-PCR on a Roche LightCycler 480 (Roche, basel, Switzerland). The total reaction volume was 20 μL, and the cycle conditions were as follows: 95 °C for 10 min, followed by 45 cycles of 95 °C for 15 s, 60 °C for 30 s, and 72 °C for 30 s. The 18S rRNA served as an internal reference for circUSP10 and USP10 mRNA, and the U6 rRNA for miR-211-5p. The $2^{-\triangle\triangle Ct}$ method was employed for relative expression calculation. The primer sequences involved in this study: circUSP10 (F:5′-CCACAAAAACCAAACAAGAGAG-3′ and R:5′-AGCACCAGTTCCCTTTATTGA-3′); TCF12 (F:5′-AGGCAGAA-CAAGCAGTACTAAT-3′ and R:5′-CACGGCTTGATGAAGAATAAGG-3′); 18S rRNA (F:5′-CGGCTACCACATCCAAGGAA-3′ and R:5′-GCTGGAATTACCGCGGCT-3′).

2.4. Agarose gel electrophoresis

The prepared PCR products were proportionally mixed with the loading buffer and sequentially added to the sample slots on an agarose gel. A DNA marker was then added to the last well. The PCR products were separated at 110 V for 43 min, and the results were observed using a gel imaging system.

2.5. RNase R assay

Total RNA from cells was incubated at 37 °C for 2 min with RNase R (Geneseed, Guangzhou, China). Enzymes from the samples were inactivated at 70 °C for 10 min. The samples were subjected to reverse transcription and qRT-PCR analyses.

2.6. Cell transfection

Cell transfection was performed using 50%–80 % confluent cells. In brief, three 1.5 mL EP tubes were prepared for each plasmid. The first tube was filled with Lipofectamine 3000 (Thermo Fisher Scientific), the second with p3000 (Thermo Fisher Scientific), and the third with the plasmid. All three sets were diluted with the basal medium and undisturbed for 5 min. Subsequently, the three agents were mixed and left undisturbed for 20 min. The mixture was added to the plate wells and mixed, and the cells were cultivated as appropriate. Knockout sequence of circUSP10: sh-circ-1: (5′-AACAAGAGAGTTGCTGGAGAA-3′); sh-circ-2 (5′-CCAAACAAGA-GAGTTGCTGGA-3′).

2.7. Cell counting Kit-8 (CCK-8) assay

After 48 h of transfection, cells were digested with pancreatin, resuspended, and counted under a microscope using a counting plate. Cells were seeded in PBS in 96-well plates (3000 cells/well) to prevent evaporation and incubated with 10 μL CCK-8 reagent for 24, 48, 72, 96, and 120 h. After 2 h, the absorbance was measured at 450 nm wavelength was determined.

2.8. Transwell assay

After 48 h of transfection, the cells were trypsinized, resuspended in a medium, and counted using a cell counting plate. Matrigel diluted with the culture medium for the cell invasion assay was plated into a chamber the previous day, incubated, and used after solidification. In brief, 600 μL of complete medium with 20 % serum was added to cells cultured in a 24-well plate, and 500 μL medium and cell suspension were placed inside the chamber. Each chamber was seeded with 5×10^4 cells for the cell migration assay, and 7×10^4 cells were used for the cell invasion assay. After being placed in the incubation for 48 h, the chambers were removed, and the cells were sequentially incubated with paraformaldehyde for 30 min and crystal violet for 15 min. Stained samples were rinsed, air-dried, photographed, and counted.

2.9. Colony formation assay

Transfected cells were seeded in a six-well plate (300 cells/well) in 1 mL of medium and cultured for 14 days. The medium was changed depending on the cell growth. Cells were examined under a microscope after gently washing each well with PBS.

2.10. 5-Ethynyl-2′-deoxyuridine (EdU) incorporation assay

The transfected cells were seeded into 48-well plates (3×10^5 cells/well). Cell proliferation was analyzed using the EdU Kit reagent (RiboBio, Guangzhou, China). After attachment to the bottom of the plate, cells were incubated with 50 μM EdU solution, stained for 2 h with Apollo and Hoechst 33342, and counted.

2.11. Nucleocytoplasmic isolation assay

Total RNA was extracted from the nucleus and cytoplasm using the Nucleocytoplasmic Isolation Kit (Beyotime, Shanghai, China). The cells were digested with pancreatin, washed twice with PBS, and probed with a cocktail of reagent A and RNase inhibitor for 10–15 min in an ice bath. The mixture was centrifuged (13000×*g* and 4 °C for 15 min) to obtain supernatant, which served as the cytoplasmic RNA sample. Subsequently, the pellet was incubated with a mixture of the reagent and RNase inhibitor in an ice bath for 30 min (20 s shaking every 1–2 min) and centrifuged (14000×*g*, 4 °C, 10 min). The supernatant was aspirated and used as the nuclear RNA fraction. Total RNA concentrations in the nucleus and cytoplasm were separately measured, and the RNA was reverse-transcribed and subjected to qRT-PCR, depending on the concentration.

2.12. RNA immunoprecipitation (RIP) assay

The RIP assay was performed according to the manufacturer's RIP Kit instructions (Bersin Bio, Guangzhou, China). Cell pellets were lysed, and the lysate was vertically mixed overnight at 4 °C with argonaute 2 (AGO2) or IgG antibody. After equilibration, the beads were vertically incubated with cell lysate spiked with AGO2 or IgG antibody for 2 h at 4 °C. Proteins were removed by treatment with the proteolytic enzyme K. A phenol, chloroform, and isoamyl alcohol mixture (25:24:1) was prepared to extract RNA, which was then subjected to qRT-PCR to evaluate circUSP10 and miR-211-5p expression levels.

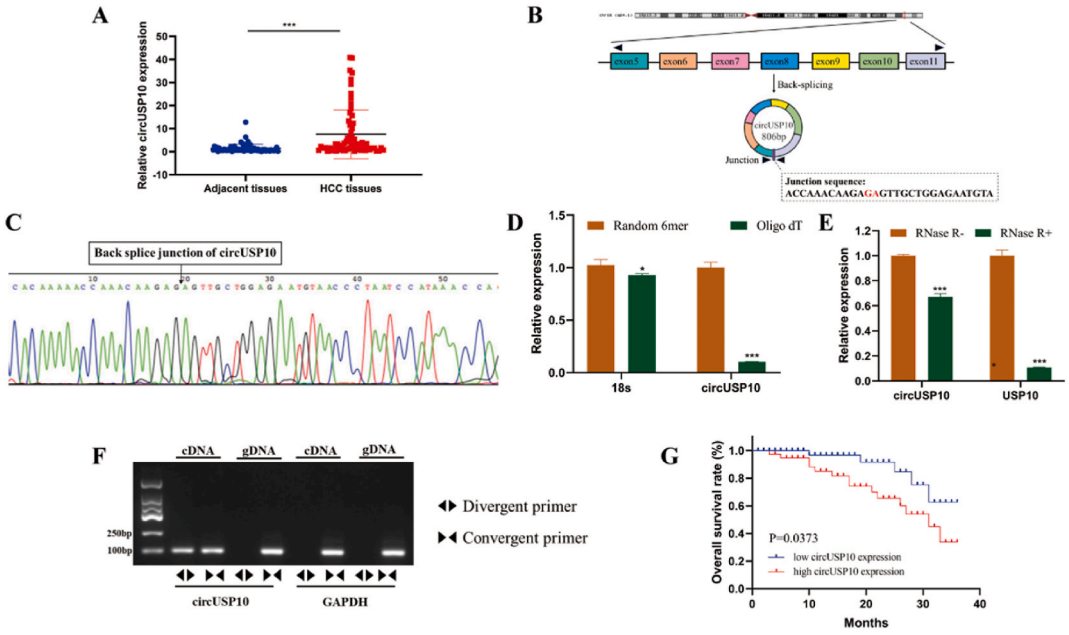

Fig. 1. Expression and cyclic structural properties of circUSP10. A. Expression of circUSP10 in 67 paired liver cancer and para-cancerous tissues. B. Expression of circUSP10 in chromosomes and its composition. C. Sanger sequencing to detect the cyclization sites of circUSP10. D. qRT-PCR assay to verify the cyclization structure of circUSP10 after reverse transcription with random 6mer and olig (dT). E. RNase R enzyme digestion to detect the stability of circUSP10. F. Agarose electrophoresis assay to verify the loop structure of circUSP10. G. Survival curve analysis to investigate the link between circUSP10 expression and prognosis of liver cancer. *: $P < 0.05$, ***: $P < 0.001$.

2.13. Dual-luciferase reporter assay

Wild-type (WT) and mutant (MUT) circUSP10 and TCF12 plasmids carrying the binding sites for miR-211-5p were designed and synthesized. These plasmids were co-transfected with miR-NC and miR-211-5p into HCCLM3 and BEL-7404 cells for 48 h. A dual-luciferase assay kit (Vazyme, Nanjing, China) was used to measure luminescence activity.

2.14. Western blot

Cells transfected for 72 h were collected and lysed in a 100:1 mixture of RIPA buffer and phenylmethylsulfonyl fluoride (PMSF; SolarBio, Beijing, China). Total protein was extracted and separated by SDS-PAGE at 80 V for 30 min, followed by 120 V for about 1 h. Following electrophoresis, the separated protein bands were transferred onto PVDF membranes at 300 mA. After blocking in a rapid blocking solution (Epizyme Biotech, Shanghai, China) for 10 min, the membranes were incubated for overnight at 4 °C with appropriate primary antibodies, including E-cadherin (1:20000, 20874-1-AP, Proteintech, Hubei, China), vimentin (1:5000, 10366-1-AP, Proteintech), N-cadherin (1:3000, 22018-1-AP, Proteintech), β-actin (1:5000, 81115-1-RR, Proteintech), TCF12 (1:5000, ab245540, Abcam, Cambridge, MA, USA), then washed with TBST, and probed with secondary antibodies for 2 h at room temperature. Detection was performed using a highly sensitive ECL chemiluminescence detection kit (Vazyme).

2.15. Hemotoxylin and eosin (H&E) staining

The liver tissues of mice were fixed with 4 % paraformaldehyde solution, embedded in paraffin, and cut into 4 μm thick slices. Afterwards, the paraffin was dissolved in xylene, rehydrated with graded ethanol, and the sections were washed and stained with hematoxylin and eosin. Stained tissue sections were observed under a light microscope and photographed.

2.16. Tumorigenesis experiments in nude mice

HCCLM3 cells were transfected with lentiviruses. Stable cell lines were obtained after treatment with puromycin. Six BALB/c nude male (4-week-old) nude mice were randomly divided into two groups. The axillae of nude mice were subcutaneously injected with approximately 1×10^7 cells, and tumor growth was observed and measured weekly. Mice were sacrificed 4 weeks later, and tumors were measured for size and weight and processed for immunohistochemistry (IHC) and H&E staining.

Table 1
Relationship of circUSP10 expression with clinicopathological features in liver cancer patients.

	Cases	circUSP10 expression		
Variables	(n = 67)	High (n = 33)	Low (n = 34)	P value
Age (year)				0.809
≤60	34	16	18	
>60	33	17	16	
Gender				0.784
Male	49	25	24	
Female	18	8	10	
HBV infection				0.776
Positive	52	25	27	
Negative	15	8	7	
Hepatocirrhosis				0.807
Present	37	19	18	
Absent	30	14	16	
Serum AFP (ng/mL)				0.615
≤200	43	20	23	
>200	24	13	11	
Tumor size (cm)				0.014*
≤5	39	14	25	
>5	28	19	9	
Tumor differentiation				0.600
Well + Moderate	46	24	22	
Poor	21	9	12	
TNM stage				0.007*
I-II	34	11	23	
III-IV	33	22	11	

*$P < 0.05$.

2.17. IHC

Nude mouse tumors were immediately fixed with paraformaldehyde after excision and embedded in paraffin. After performing a series of operations, such as sectioning, dewaxing in water, antigen repair, closure, antibody incubation, color development, and nuclear re-staining, the samples were observed, and images were acquired using a microscope.

2.18. Bioinformatics analyses

The miRNA downstream of circUSP10 was searched through circbank (http://www.circbank.cn/) and starbase (https://starbase.sysu.edu.cn/) databases, and the mRNA downstream of miR-211-5p was searched through miRTarBase (https://maayanlab.cloud/Harmonizome/resource/MiRTarBase), TargetScan (https://www.targetscan.org/vert_71/), miRDB (https://mirdb.org/index.html) and ENCORI (https://starbase.sysu.edu.cn/) databases. A Venn diagram was drawn by cross-analysis using the Evenn database (http://www. ehbio. com/test/venn/#/).

2.19. Statistical analysis

Statistical analyses were conducted using SPSS Statistics 23.0 and GraphPad Prism 8.0.2. Fisher's exact test determined the correlation between circUSP10 expression and the clinicopathological parameters. Survival analysis was performed using the Kaplan-Meier method. Comparisons were performed using a *t*-test and one-way analysis of variance (ANOVA). $P < 0.05$ indicates statistical significance.

3. Results

3.1. CircUSP10 expression is upregulated in LC and related to LC progression

Appropriate circRNAs were screened from published gene chips of LC in the GEO database. In the GSE97332 dataset, we used $|\log FC| > 2$ and $P < 0.05$ to filter and draw the heat map (SFig. 1). RT-qPCR revealed high circUSP10 expression in 67 pairs of LC tissue samples (Fig. 1A). Hence, we selected circUSP10 for follow-up studies.

In the circBank database, circUSP10 is located at chr16:84792321–84801964, which is formed by the shear cyclization of exons 5–11 of USP10 (Fig. 1B). We then sequenced the qRT-PCR product of circUSP10 by sanger method and found that the "GA" site was the cyclization site of circUSP10 (Fig. 1C). As circRNAs lack poly(A) tails, we reverse-transcribed them with oligo (dT) or random 6-mers and detected their expression by qRT-PCR (Fig. 1D). CircUSP10 can be transcribed by random 6-mers, but not by oligo (dT), indicating that it exhibits an intact closed-loop structure. We then treated total cellular RNA with RNase R. We conducted qRT-PCR (Fig. 1E),

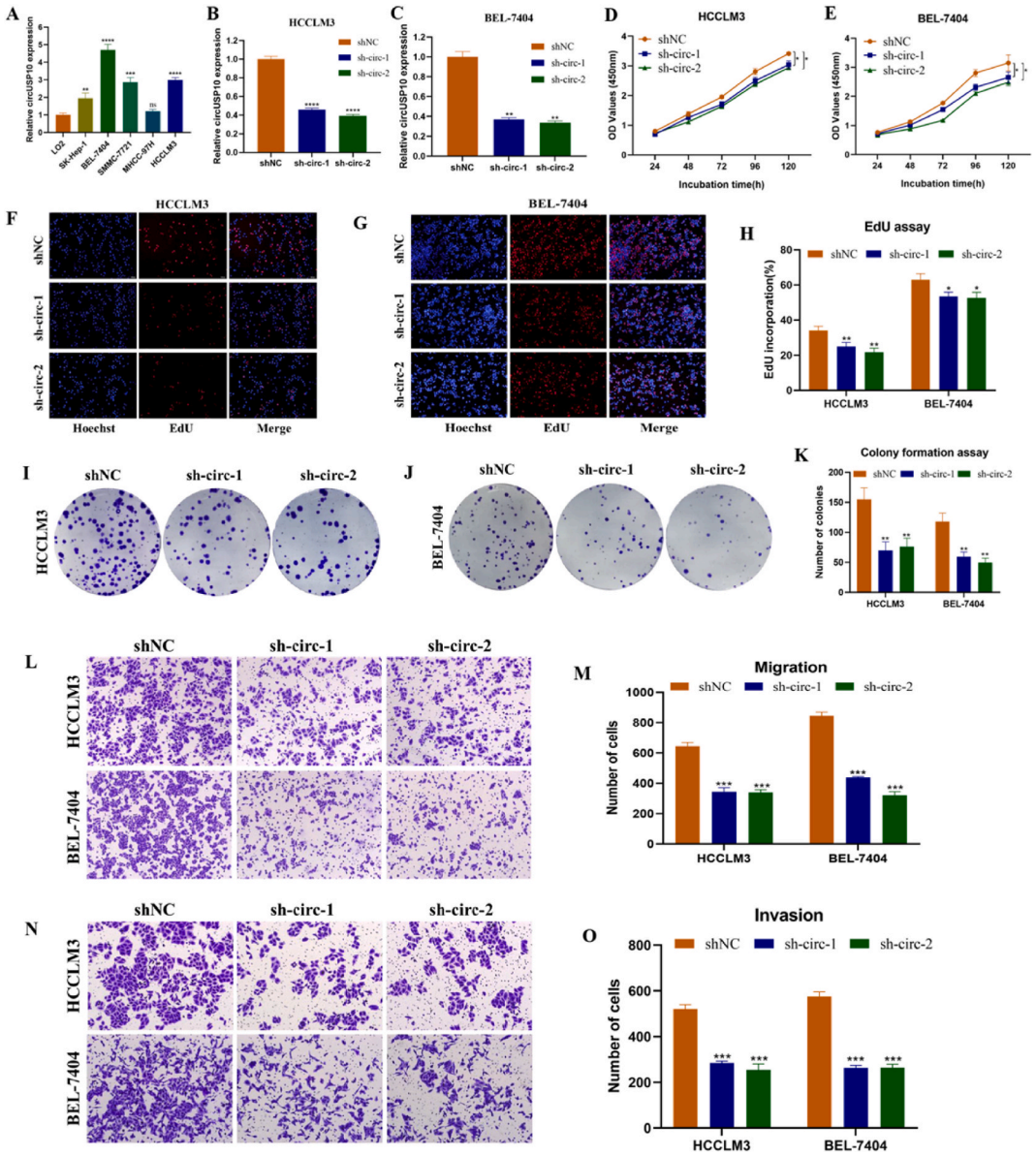

Fig. 2. Effect of knockdown of circUSP10 expression on liver cancer cell properties. A. circUSP10 expression in liver cancer cells. B and C. Evaluation of knockdown efficiency of circUSP10 in HCCLM3 and BEL-7407 cell lines. D–K. CCK-8 (D and E), EdU (F–H), and colony formation (I–K) assays with HCCLM3 and BEL-7407 cells after knockdown of circUSP10. L–O. Transwell migration (L and M) and invasion (N and O) assays with HCCLM3 and BEL-7407 cells after circUSP10 expression knockdown. *: $P < 0.05$, **: $P < 0.01$, ***: $P < 0.001$.

which showed that USP10, the linear parent gene of circUSP10, had significantly decreased expression and circUSP10 expression remained unchanged. Thus, circUSP10 exhibits good stability. We then designed divergent and convergent primers for circUSP10 and performed agarose gel electrophoresis. Only circUSP10 was amplified using both primer types in the presence of cDNA as a template (Fig. 1F). This observation further confirms the circular structure of circUSP10.

According to the analysis of clinicopathological data from 67 patients with LC, circUSP10 expression correlated with tumor size and tumor node metastasis (TNM) stage (Table 1). We plotted overall survival (OS) curves and found significantly higher OS rates among patients with low circUSP10 expression than those with high circUSP10 levels (Fig. 1G).

In summary, circUSP10 is a cyclic RNA overexpressed in LC, and its expression correlates with the tumor size and TNM stage of patients. Thus, it can be a stable, clinically valuable diagnostic and prognostic indicator.

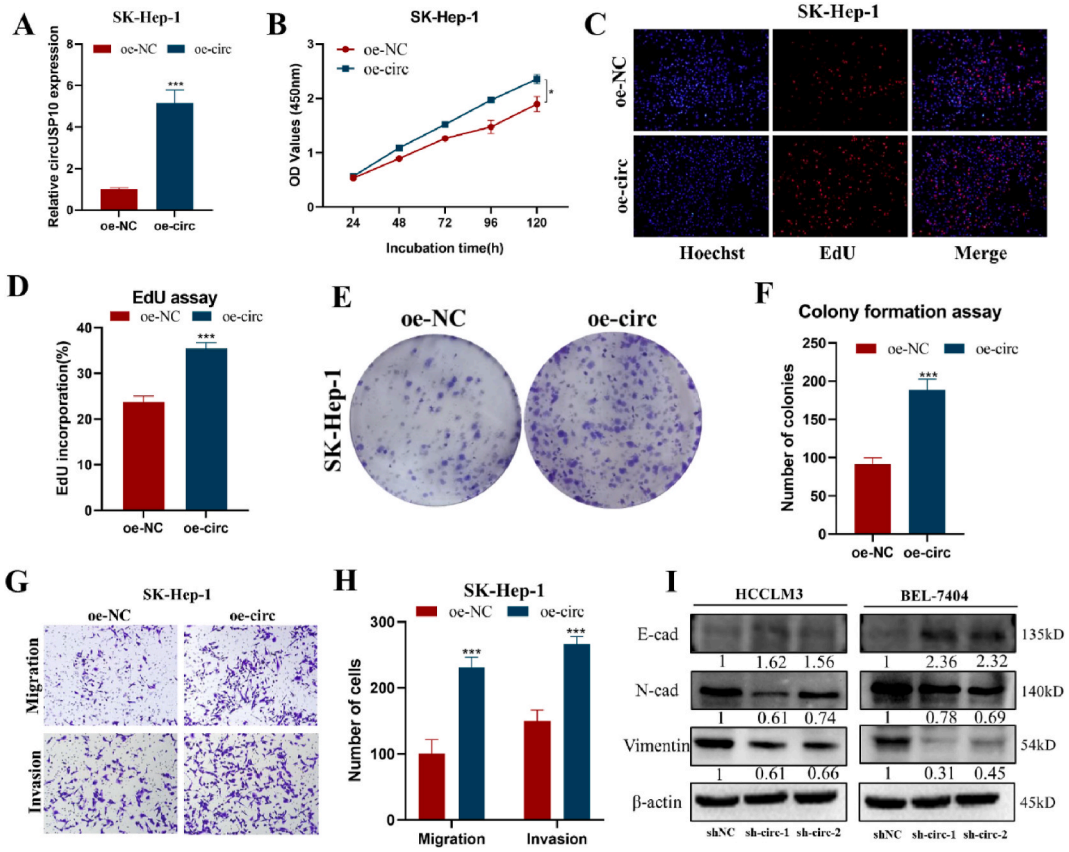

Fig. 3. Effects on liver cancer cell properties after circUSP10 overexpression and the relationship between circUSP10 and EMT pathway proteins. A. Overexpression efficiency of circUSP10 in SK-Hep-1 cells. B–F. CCK-8 (B), EdU (C–D), and colony formation (E–F) assays were performed in SK-Hep-1 cells after overexpression of circUSP10. G and H. Transwell migration and invasion assays were performed in SK-Hep-1 cells after overexpression of circUSP10 (G and H). I. Western blotting to study the effect of circUSP10 knockdown on EMT pathway proteins. *: $P < 0.05$, ***: $P < 0.001$.

3.2. CircUSP10 promotes the growth and metastasis of LC cells and is related to the EMT pathway

We explored the effects of circUSP10 on the tumorigenic characteristics of LC cells using in vitro functional assays. First, we investigated circUSP10 expression by qRT-PCR. We found significantly higher levels in SK-Hep-1, BEL-7404, SMMC-7721, MHCC-97H, and HCCLM3 cells than in the normal hepatocyte line, LO2 (Fig. 2A). The expression of circUSP10 was highest in BEL-7404 cells, followed by HCCLM3 cells, and was lowest in SK-Hep-1 cells. Therefore, we performed interference experiments using BEL-7404 and the HCCLM3 cell lines and overexpression experiments using the SK-Hep-1 cell line.

We constructed interference vectors and verified transfection efficiency by microscopic fluorescence observation (SFig. 2) and qRT-PCR. CircUSP10 expression was significantly lower in the knockdown group (sh-circ-1 and sh-circ-2) than that in the control (shNC) (Fig. 2B and C). CCK-8 assay results revealed that BEL-7404 and HCCLM3 cells showed significantly decreased proliferation after circUSP10 knockdown (Fig. 2D and E). The EdU experiment also highlighted the significant decrease in the proportion of proliferating cells in the sh-circ-1 and sh-circ-2 treatment groups compared to the shNC treatment group (Fig. 2F–H). In the colony formation assay, the number of colony-forming units was significantly lower in the group transfected with the interfering vector than in the control (Fig. 2I–K). These results suggest that circUSP10 is associated with LC cell proliferation. In the Transwell migration assay, the migration ability of cells in the sh-circ-1 and sh-circ-2 treatment groups was lower than that in the shNC treatment group (Fig. 2L and M). Furthermore, in the cell invasion assay, the invasive ability of cells was reduced after circUSP10 knockdown (Fig. 2N and O). In conclusion, the results of the transwell assays indicated that circUSP10 expression was associated with cell metastasis.

We constructed overexpression vectors (oe-circ) and verified their transfection efficiency using qRT-PCR (Fig. 3A). CCK-8, EdU, and clone formation assay results revealed a significantly higher proliferative ability of cells overexpressing circUSP10 than that of control cells (Fig. 3B–F). Migration and invasion assays also demonstrated increased cell migration and invasion after circUSP10 overexpression (Fig. 3G and H).

As circUSP10 promotes LC cell migration and invasion, we investigated whether its expression is associated with the EMT pathway. Western blotting results confirmed the elevation in E-cadherin expression and the decrease in N-cadherin and vimentin expression after the dysregulation of circUSP10 expression (Fig. 3I).

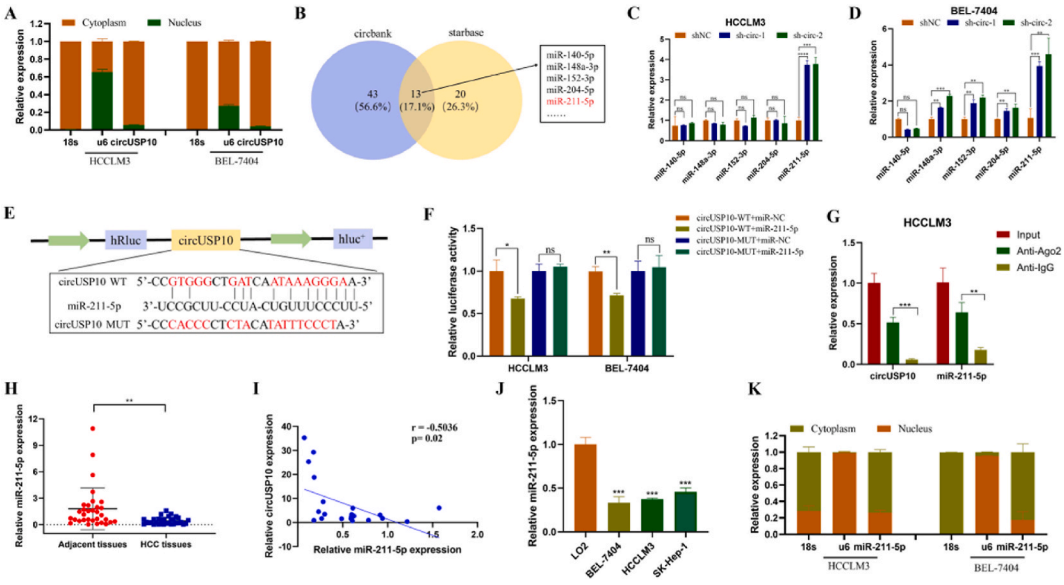

Fig. 4. CircUSP10 adsorbs and binds to miR-211-5p. A. Nucleocytoplasmic isolation assay of circUSP10 in HCCLM3 and BEL-7407 cells. B. Database-dependent prediction of miRNAs that can bind to circUSP10. C and D. qRT-PCR detected changes in each miRNA expression after the knockdown of circUSP10 expression in HCCLM3 and BEL-7407 cells. E. Construction of MUT and WT circUSP10 and miR-211-5p binding sites. F. Dual-luciferase assay to verify circUSP10 and miR-211-5p binding. G. RIP assay in HCCLM3 cells and circUSP10 and miR-211-5p enrichment analysis. H. qRT-PCR to detect miR-211-5p in 32 paired liver cancer and para-cancerous tissues. I. Correlation analysis between miR-211-5p and circUSP10. J. Detection of miR-211-5p in liver cancer cells by qRT-PCR. K. Nucleocytoplasmic isolation assay of miR-211-5p in HCCLM3 and BEL-7407 cells. *: $P < 0.05$, **: $P < 0.01$, ***: $P < 0.001$.

Together, these results confirmed that circUSP10 promotes the tumorigenic properties of LC cells and is associated with the EMT pathway.

3.3. CircUSP10 can adsorb miR-576-5p in LC

circRNAs contain several miRNA-binding sites and can enhance the expression of target genes by adsorbing miRNAs, thus relieving the repressive effects of miRNAs on their target genes [22]. Such circRNAs are competitive endogenous RNAs (ceRNAs), mainly located in the cytoplasm. Therefore, we performed nucleoplasmic separation experiments using HCCLM3 and BEL-7404 cells and found that circUSP10 was mainly expressed in the cytoplasm (Fig. 4A). We then searched for miRNA molecules that might bind to circUSP10 in CircBank and starBase. We performed Venny analysis (Fig. 4B). Thirteen common miRNAs were identified in both databases (miR-670-3p, miR-1245b-5p, miR-1269a, miR-140-5p, miR-148a-3p, miR-148b-3p, miR-152-3p, miR-204-5p, miR-211-5p, miR -2681-3p, miR-3142, miR-3690, and miR-378h). Previous studies have reported downregulation of miR-140-5p [23], miR-148b-3p [24], miR-152-3p [25], miR-204-5p [26], and miR-211-5p [27] in LC tissues. Only miR-211-5p expression was significantly increased following circUSP10 knockdown in HCCLM3 cells, whereas the other four candidates were upregulated after circUSP10 knockdown in BEL-7404 cells (Fig. 4C and D). Hence, we speculated that miR-211-5p may serve as a circUSP10 target. Next, we constructed WT and MUT circUSP10 (Fig. 4E) and verified whether miR-211-5p is bound to these circRNAs. The results showed that the luminescence signal in the WT group was lower after co-transfection with miR-211-5p and circUSP10-WT than in the control group (circUSP10-WT + miR-NC). In the MUT group, the luciferase activity of the control (circUSP10-MUT + miR-NC) and experimental (circUSP10-MUT + miR-211-5p) groups was approximately the same (Fig. 4F). CircRNAs and miRNAs bind to AGO2 molecules, which are indicator proteins for circRNAs that exert sponge actions [28]. The results of the RIP experiments showed that compared with the negative control IgG, the anti-Ago2 antibody effectively pulled down circUSP10 and miR-211-5p (Fig. 4G). These results confirmed that circUSP10 binds to miR-211-5p and functions as a miRNA sponge via AGO2.

We verified miR-211-5p expression using qRT-PCR and found it downregulated in 32 pairs of LC tissues (Fig. 4H). In addition, miR-211-5p expression negatively correlated with circUSP10 expression (Fig. 4I). MiR-211-5p expression was downregulated in LC cells (Fig. 4J), and a nucleocytoplasmic isolation assay confirmed miR-211-5p aggregation, similar to that of circUSP10, mainly in the cytoplasm (Fig. 4K).

These results revealed that circUSP10 can regulate miR-211-5p expression by acting as a sponge.

3.4. MiR-211-5p is a downstream target of circUSP10 and inhibits LC cell growth and metastasis

Based on these results, we hypothesized that miR-211-5p inhibited LC development. We constructed miR-211-5p mimics and

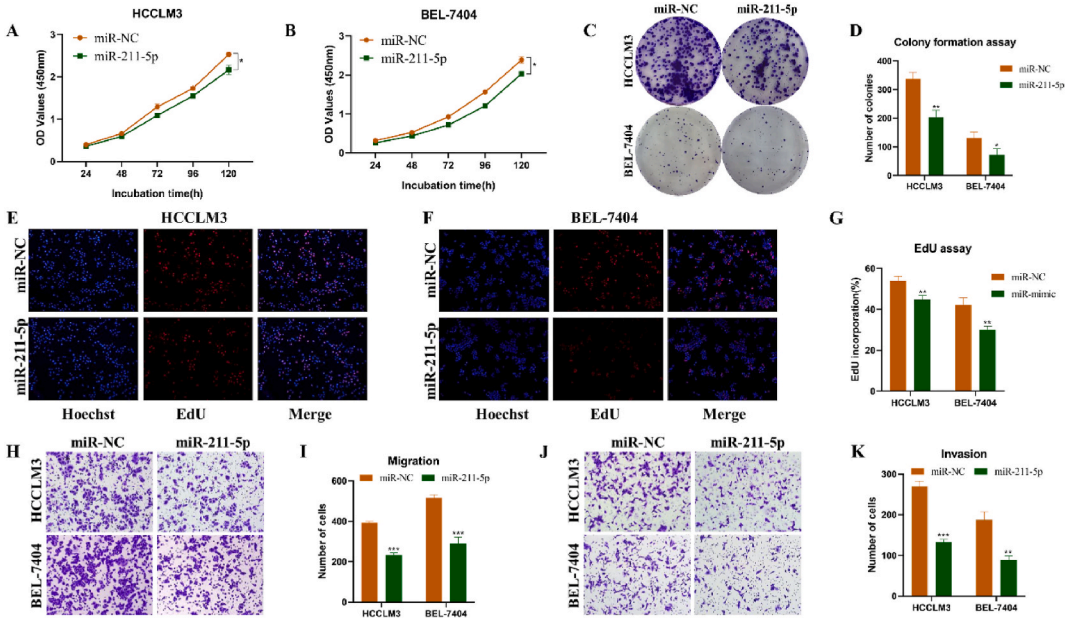

Fig. 5. Effect of miR-211-5p on tumorigenic properties of liver cancer cells. A–G. CCK-8 (A and B), colony formation (C and D), and EdU (E–G) assays with HCCLM3 and BEL-7407 cells after transfection of miR-211-5p mimics. H–K. Transwell migration (H and I) and invasion (J and K) assays with HCCLM3 and BEL-7407 cells following miR-211-5p mimic transfection. *: $P < 0.05$, **: $P < 0.01$, ***: $P < 0.001$.

performed in vitro experiments. CCK-8, clone formation, and EdU assays showed that the proliferative ability of the cells decreased after miR-211-5p mimic (miR-211-5p) transfection compared to the control (miR-NC) transfection (Fig. 5A–G). Thus, miR-211-5p suppressed the growth of LC cells. In the Transwell assay, cell migration and invasion were decreased in the miR-211-5p group compared to those in the miR-NC group (Fig. 5H–K). Thus, miR-211-5p inhibits LC cell metastasis.

3.5. TCF12, a target molecule of miR-211-5p, binds to miR-211-5p and is upregulated in LC

To further explore the ceRNA effects of circUSP10, we predicted the miR-211-5p target genes using four databases: miRTarBase, TargetScan, miRDB, and ENCORI. We constructed a Venn diagram and identified three common intersections: TCF12, CREB5, and ELOVL6 (Fig. 6A). The relationship of miR-211-5p with these three molecules was further analyzed using the ENCORI database; TCF12 and CREB5 were found to be negatively correlated, and ELOVL6 was positively correlated with miR-211-5p (Fig. 6B). The expression of TCF12 and CREB5 in LC was predicted using the TIMER database. Compared to the normal group, the expression of TCF12 and CREB5 in the tumor group was relatively increased, and the differential expression of TCF12 was more significant (Fig. 6C). Next, we verified the correlation between TCF12, CREB5, and miR-211-5p in the two cell lines (Fig. 6D and E). TCF12 expression was lower in cells treated with miR-211-5p mimics than in cells transfected with control miR-NC. No significant changes were observed in the CREB5 levels. Then, we transfected the circUSP10 interference vector and observed changes in TCF12 expression. We found significantly lower levels of TCF12 after sh-circ-1 and sh-circ-2 treatment than after the control shNC treatment (Fig. 6F). Therefore, we hypothesized that TCF12 functions downstream of miR-211-5p. We designed WT and MUT sequences of TCF12 and constructed vectors for the dual-luciferase reporter assay (Fig. 6G). The luciferase activity of the WT was significantly decreased in the experimental group (TCF12+miR-211-5p) compared to that in the control group (TCF12+miR-NC). However, no significant variation was observed in the MUT group (Fig. 6H). Therefore, we inferred that TCF12 binds to miR-211-5p. We found that TCF12 expression was upregulated in 35 pairs of LC tissues and cell lines (Fig. 6I and J) and, positively correlated with circUSP10 (Fig. 6K), and negatively correlated with miR-211-5p (Fig. 6L).

Western blotting revealed decreased TCF12 protein levels after transfection with the circUSP10 interference vector (Fig. 6M). Compared with miR-NC, miR-211-5p mimics decreased TCF12 expression, approximately the same after co-transfection of miR-211-5p mimics with oe-NC as only transfection of miR-211-5p mimics. Compared with miR-211-5p + oe-NC, the expression of TCF12 was increased again after miR-211-5p + oe-circ co-transfection (Fig. 6N).

Overall, the above experimental results demonstrate that circUSP10 is a ceRNA that regulates miR-211-5p and, therefore, TCF12 expression.

3.6. CircUSP10 promotes LC cell growth and metastasis via regulation of miR-211-5p/TCF12/EMT signaling

To investigate whether circUSP10 promotes LC progression via miR-211-5p–mediated TCF12 expression, we designed a TCF12 overexpression vector (OE) and verified its transfection efficiency at the mRNA and protein levels (Fig. 7A and B). CCK-8, EdU, and

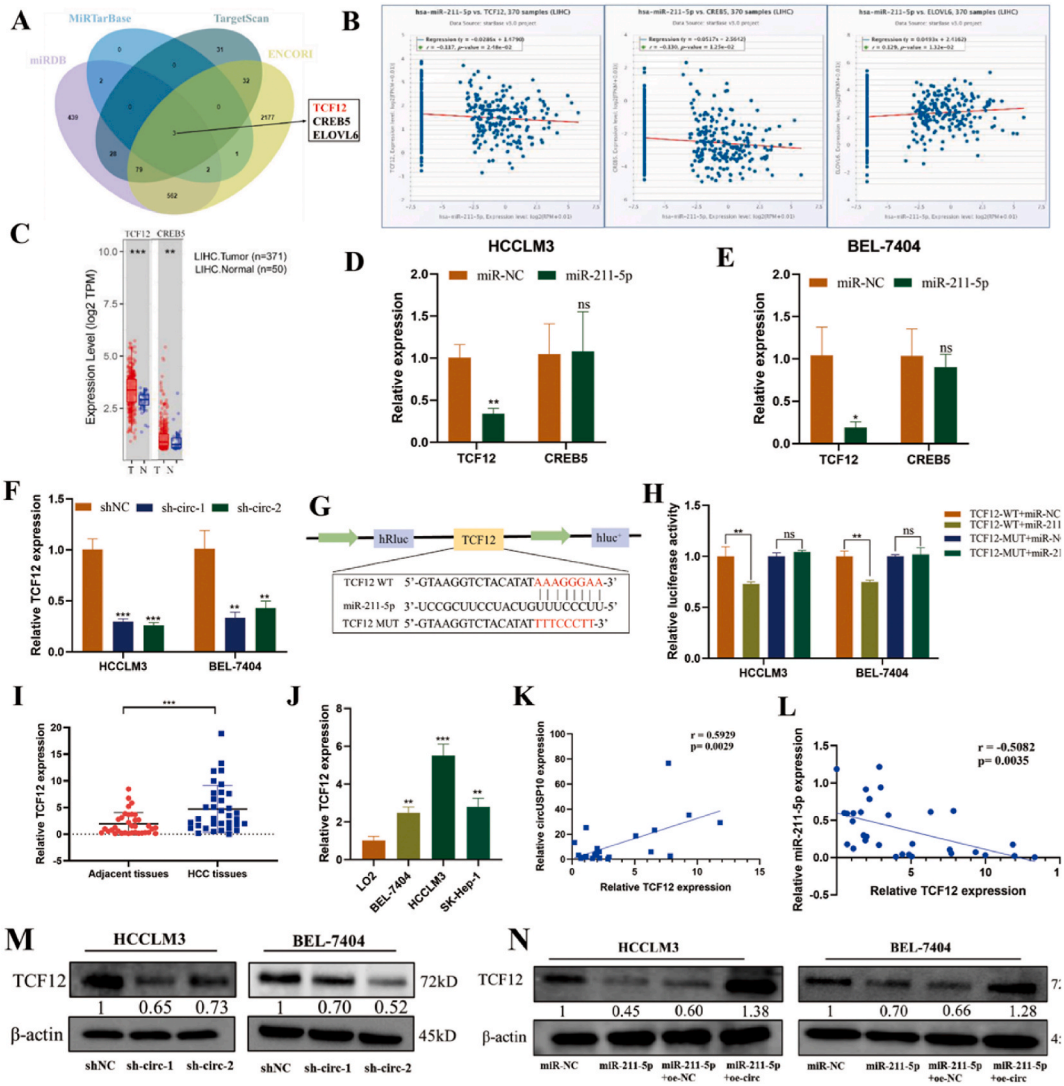

Fig. 6. TCF12 is a target molecule acting downstream of miR-211-5p. A. Screening of mRNAs that can potentially bind to miR-211-5p from the database and plotting of Venny diagram. B. Prediction of correlation between miR-211-5p and mRNAs from the ENCORI database. C. Analysis of CREB5 and TCF12 expression in liver cancer from the TIMER database. D and E. After overexpression of miR-211-5p in HCCLM3 and BEL-7407 cells, TCF12 and CREB5 expression was analyzed by qRT-PCR. F. qRT-PCR detected TCF12 expression after knockdown of circUSP10 expression. G. Construction of WT and MUT sequences of TCF12 with an miR-211-5p binding site. H. Verification of the binding of TCF12 to miR-211-5p. I and J. qRT-PCR to validate TCF12 expression in liver cancer tissues and cells. K. TCF12 correlation analysis with circUSP10. L. miR-211-5p correlation analysis with TCF12. M. Western blotting to determine changes in TCF12 protein levels after knockdown of circUSP10 expression in HCCLM3 and BEL-7407 cells. N. Changes in TCF12 protein following transfection of miR-NC, miR-211-5p, miR-211-5p + oe-NC, or miR-211-5p + oe-circ in HCCLM3 and BEL-7407 cells. *: $P < 0.05$, **: $P < 0.01$, ***: $P < 0.001$.

clone formation assay results demonstrated an increase in LC cell proliferation after TCF12 overexpression compared to the control (nc), and this effect was reversed following co-transfection of miR-211-5p mimics and the TCF12 overexpression vector. Continuous addition of the circUSP10 overexpression vector led to further escalation of cell proliferation (Fig. 7C–I). In the transwell assay, the oe group showed enhanced migration and invasion compared to the nc group, but co-transfection with oe and miR-211-5p led to suppressive effects on these properties. However, these properties were enhanced in cells co-transfected with oe + miR-211-5p + oe-circ (Fig. 7J–M).

Based on this grouping, we validated the functions of circUSP10, miR-211-5p, and TCF12 in EMT. Compared to the NC group, the OE group showed augmented N-cadherin and vimentin levels. N-cadherin and vimentin expression were suppressed after oe + miR-211-5p co-transfection; however, their levels were elevated in the oe + miR-211-5p + oe-circ co-transfection group. The expression of E-cadherin showed the opposite trend to that of N-cadherin and vimentin (Fig. 7N).

CircUSP10 promotes LC cell tumorigenic properties by regulating miR-211-5p-mediated TCF12 expression and is relevant to the

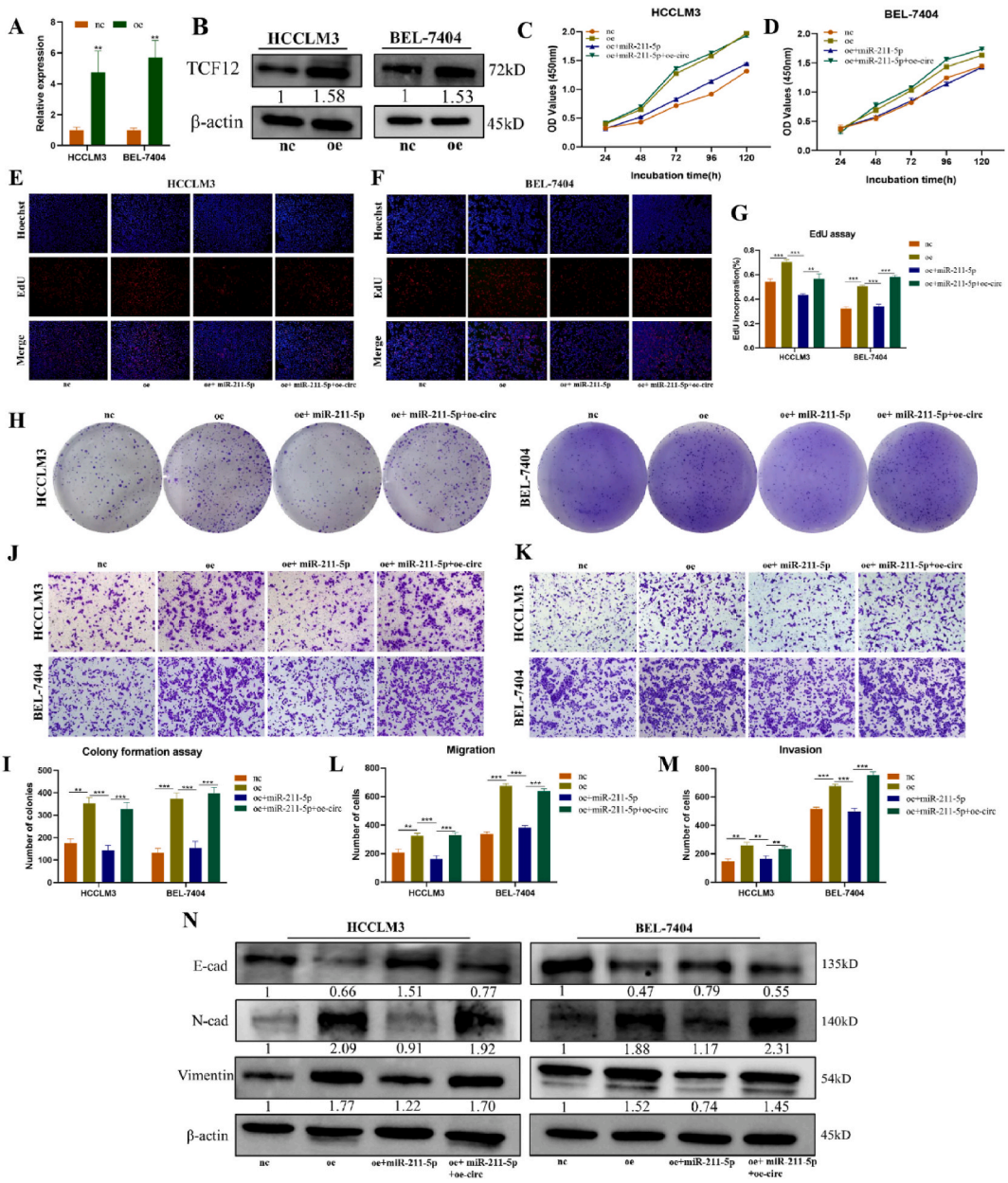

Fig. 7. CircUSP10 promotes liver cancer growth and metastasis through miR-211-5p/TCF12/EMT. A and B. TCF12 mRNA and protein expression in response to TCF12 overexpression in HCCLM3 and BEL-7407 cells. C–I. CCK-8 (C and D), EdU (E–G), colony formation (H and I) assays, and Transwell migration and invasion assay (J–M) after transfection of nc, oe, oe + miR-211-5p, or oe + miR-211-5p + oe-circ in HCCLM3 and BEL-7407 cells. N. Changes in EMT pathway-related proteins in HCCLM3 and BEL-7407 cells under different transfection conditions were detected by western blotting. **: $P < 0.01$, ***: $P < 0.001$.

EMT pathway.

3.7. CircUSP10 expression knockdown in nude mice leads to tumor growth inhibition

To explore the influence of circUSP10 on tumors in vivo, we constructed lentiviral knockdown vectors (shNC and sh-circ) for circUSP10. Stably transfected HCCLM3 cells were administered to the axillae of nude mice. Tumor weight and volume were recorded every 7 days and were markedly lower in the sh-circ group than in the shNC group (Fig. 8A-D). Twenty-eight days later, the mice were euthanized, and the excised tumor samples were subjected to H&E staining and IHC. The IHC results demonstrated lower protein levels of Ki67, PCNA, and vimentin in the sh-circ group than in the shNC group (Fig. 8E). These results, as well as the in vitro findings, suggest

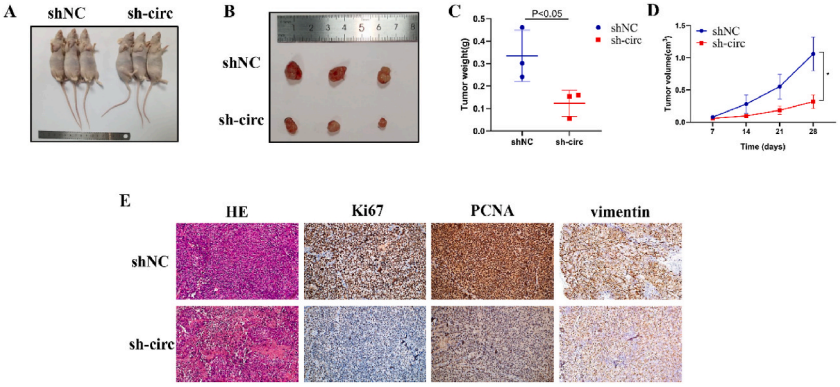

Fig. 8. Knockdown of circUSP10 inhibits growth of tumor in nude mice in vivo. A-B. Tumor growth after 28 days. C. Tumor weight statistics in shNC and sh-circ groups. D. Tumor volume changes of nude mice in shNC and sh-circ groups were recorded every 7 days. E. H&E staining and immunohistochemistry were performed to detect Ki67, PCNA and vimentin protein expression in shNC and sh-circ groups. *: $P < 0.05$.

that circUSP10 inhibits tumor growth via EMT in vivo.

4. Discussion

The pathogenesis of LC is complex and involves epigenetic alterations, abnormal expression of oncogenes and tumor suppressors, changes in cell cycle protein levels and activities, modified apoptosis, pathological angiogenesis, and dysregulated immune monitoring [29]. Hepatitis virus infection, fatty liver, environmental factors, and unhealthy lifestyle are predisposing factors for LC [30]. Currently, the diagnosis of LC can be confirmed by blood biomarkers combined with imaging examinations, but these methods lack sensitivity and specificity in the early stages of LC [31]. To date, some questions remain regarding the theory of LC; therefore, the exact molecules and signaling pathways involved in the occurrence and development of LC remain to be elucidated.

CircRNAs are a class of ncRNAs, most of which are closed-loop structures formed by exons [32]. Due to their unique structure, circRNAs can stably exist in body fluids, cells, and tissues. The expression of hsa_circ_0015286 is significantly increased in the tissues, plasma, and cell lines of patients with gastric cancer (GC). It is associated with tumor size, TNM stage, and lymph node metastasis. After surgical treatment, the expression of plasma hsa_circ_0015286 was significantly lower than before surgery, and GC patients with high hsa_circ_0015286 expression had a worse prognosis. Plasma hsa_circ_0015286 may be used as a noninvasive biomarker to assist in the diagnosis and prognosis of GC [33]. The expression of circ_001680 in colorectal carcinoma (CRC) tissues is higher than that in adjacent tissues, which affects the proliferation and migration of CRC cells and is related to resistance to irinotecan treatment [34]. We identified an association between circRNAs and LC. For example, circ-100395, circ-0039459, and circ-CSPP1 are aberrantly expressed in LC and associated with cancer cell proliferation, apoptosis, migration, and invasion [35–37]. Hence, we speculate that circRNAs are involved in the process of LC and can act as biomarkers for the diagnosis, treatment, and prognosis of LC.

Here, we filtered a circRNA, circUSP10, upregulated in LC from the GEO database. CircUSP10, composed of exons 5–11, is resistant to digestion by RNase R and has a stable closed-loop structure. Clinicopathological data showed that circUSP10 was associated with tumor size and TNM stage and that higher circUSP10 levels corresponded to shorter OS in patients with LC. This suggests that high circUSP10 expression is associated with a poor prognosis and may be used as a clinical marker to assist in the diagnosis and prognosis of LC. In vitro cell function experiments, the CCK-8, EdU, and colony formation assays confirmed that circUSP10 was associated with the growth of LC cells, and transwell migration and invasion assays showed that circUSP10 was related to the metastasis of LC cells. In vivo experiments in nude mice also demonstrated that circUSP10 promoted tumor growth. Thus, we postulated that circUSP10 promotes LC development and could be a diagnostic and prognostic marker for LC.

We investigated its biological role in LC and found that CircUSP10 is composed of exons mainly localized in the cytoplasm, suggesting its role in sponging miRNAs. Bioinformatics predicted that miR-211-5p might be the downstream target of circUSP10, and RIP and dual-luciferase experiments proved that circUSP10 could act as a sponge by adsorbing miR-211-5p. We also confirmed that the overexpression of miR-211-5p suppressed LC cell proliferation, migration, and invasion. Additionally, miR-211-5p has been proposed to impede the tumorigenic properties of thyroid tumor cells through negative SOX11 regulation [38]. Li et al. [39] found that circNRIP1 knockdown promotes ovarian cancer sensitivity to paclitaxel via the miR-211-5p/HOXC8 axis, further validating the role of circRNA-miRNAs in tumors.

TCF12, also known as HTF4 or HEB, is a member of the HLH protein family [40]. TCF12 is widely expressed in various tissues and cells of the body, such as skeletal muscle, thymus, and B cells. It is involved in gene transcription, regulation of T cell development, basal cell generation, and mesenchymal cell differentiation [41]. TCF12 is associated with tumors and can play an oncogenic role in colorectal and gallbladder cancer; however, it prevents tumor growth in prostate cancer [42–44]. Herein, we demonstrate the existence of binding sites for miR-211-5p and TCF12. TCF12 mRNA and protein expression decrease following circUSP10 knockdown. TCF12 principally acts as a promoter of LC. In a triple-reply experiment, circUSP10, miR-211-5p, and TCF12 interacted with each other, and miR-211-5p inhibited the promotive action of TCF12 on LC, which was diminished in the presence of circUSP10.

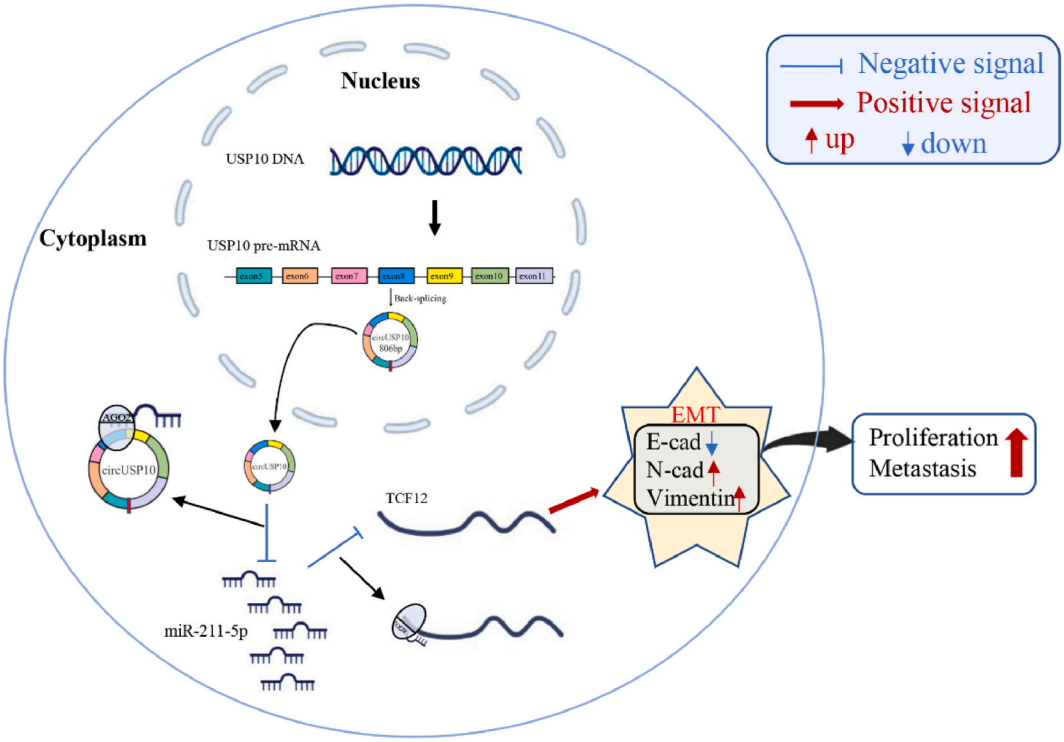

Fig. 9. Mechanistic sketch of the role of circUSP10 in LC.

EMT refers to the reduction in tight and adherent junctions between epithelial cells in response to several factors and the acquisition of the ability to infiltrate and migrate [45]. In parallel with the changes in cell phenotype, the expression of some proteins was altered. For example, a decrease in the expression level of E-cadherin can lead to a reduction in cell adhesion, making cells more prone to invasion and metastasis [17]. Among these, the loss of E-cadherin expression has been recognized as the most prominent feature of EMT [46]. Simultaneously, the cells acquired a mesenchymal phenotype, such as increased expression of vimentin and N-cadherin [47]. CircRNAs can affect tumor development through the EMT pathway. The expression of circESRP1 is increased in endometrial cancer (EC), affecting the expression of vimentin and E-cadherin and regulating the EMT pathway through the miR-874-3p/CPEB4 axis to affect EC metastasis [48]. Additionally, TCF12 is associated with the EMT pathway. HDAC1 promotes the migration and invasion of gallbladder cancer cells by binding to TCF12, thereby promoting EMT [43]. In addition, miR-154 regulated by wt-p53 could inhibit the migration, invasion, and EMT of glioblastoma multiforme cells by targeting TCF12 [49]. Here, the knockdown of circUSP10 expression was followed by corresponding changes in E-cadherin, N-cadherin, and vimentin expression, consistent with the alterations in these protein levels in the circUSP10/miR-211-5p/TCF12 triple-reply assay.

Our study has some limitations. First, there may be other sequencing chips in the GEO database; therefore, we cannot exclude other circRNA molecules that may be highly expressed in LC, and these circRNAs may play a role in the progression of LC. Second, in this study, the expression of circUSP10 was only detected in the tissues of patients with LC, and the feasibility of circUSP10 as a diagnostic marker of LC can be further elucidated by detecting circUSP10 in patients' blood. Finally, the other mechanisms circUSP10 participates in LC progression remain to be elucidated. Therefore, the role of circUSP10 in LC requires further investigation.

5. Conclusion

In summary, circUSP10 was overexpressed in LC and promoted cancer progression by regulating the miR-211-5p/TCF12/EMT pathway. These findings provide new insights into the clinical diagnosis and prognosis of LC (Fig. 9).

Ethical approval and informed consent statement

The clinical samples were collected from patients after informed consent was obtained. This study was performed with the approval of the Ethics Committee of the Affiliated Hospital of Nantong University (the approval number: 2019-L071). The animal experiments involved in this study were approved by the Laboratory Animal Center of NTU (the animal ethics approval number: S20200323-150)

Data availability statement

The dataset supporting the conclusions of this article is included within this article and is available from the corresponding author upon request.

Funding

This work was financially supported by Nantong Science and Technology Project (MS22021001), Suzhou Special project of diagnosis and treatment technology for key clinical diseases (LCZX202204).

CRediT authorship contribution statement

Xiang Chen: Conceptualization, Data curation, Methodology, Project administration, Software, Supervision, Validation, Writing – original draft. **Yao Xu:** Conceptualization, Investigation, Methodology, Software, Validation, Writing – original draft. **Zhengyang Zhou:** Investigation, Methodology, Software. **Ping Zhao:** Investigation, Methodology, Software, Validation. **Zhou Zhou:** Investigation, Methodology, Software, Validation. **Feng Wang:** Investigation, Methodology, Software, Validation. **Fengyun Zhong:** Funding acquisition, Supervision, Validation, Writing – review & editing. **Hong Du:** Funding acquisition, Supervision, Validation, Writing – review & editing.

Declaration of competing interest

The authors declare that they have no known competing financial interests or personal relationships that could have appeared to influence the work reported in this paper.

Appendix A. Supplementary data

Supplementary data to this article can be found online at https://doi.org/10.1016/j.heliyon.2023.e20649.

References

[1] H. Sung, J. Ferlay, R.L. Siegel, M. Laversanne, I. Soerjomataram, A. Jemal, F. Bray, Global cancer statistics 2020: GLOBOCAN estimates of incidence and mortality worldwide for 36 cancers in 185 countries, CA, Cancer. J. Clin. 71 (2021) 209–249, https://doi.org/10.3322/caac.21660.
[2] S. Chidambaranathan-Reghupaty, P.B. Fisher, D. Sarkar, Hepatocellular carcinoma (HCC): epidemiology, etiology and molecular classification, Adv. Cancer Res. 149 (2021) 1–61, https://doi.org/10.1016/bs.acr.2020.10.001.
[3] Z. Kang, K. Jin, J. Jing, The value of MRI combined with AFP, AFP-L3, GP73, and DCP in the diagnosis of early primary liver cancer, Dis. Markers 2022 (2022), 8640999, https://doi.org/10.1155/2022/8640999.
[4] Y. Zheng, M. Zhu, M. Li, Effects of alpha-fetoprotein on the occurrence and progression of hepatocellular carcinoma, J. Cancer Res. Clin. Oncol., https://doi.org/10.1007/s00432-020-03331-6.
[5] H. Hanif, M.J. Ali, A.T. Susheela, I.W. Khan, M.A. Luna-Cuadros, M.M. Khan, D.T. Lau, Update on the applications and limitations of alpha-fetoprotein for hepatocellular carcinoma, World, J. Gastroenterol. 28 (2022) 216–229, https://doi.org/10.3748/wjg.v28.i2.216.
[6] C.Y. Yu, H.C. Kuo, The emerging roles and functions of circular RNAs and their generation, J. Biomed. Sci. 26 (2019) 29, https://doi.org/10.1186/s12929-019-0523-z.
[7] S. Meng, H. Zhou, Z. Feng, Z. Xu, Y. Tang, P. Li, M. Wu, CircRNA: functions and properties of a novel potential biomarker for cancer, Mol. Cancer 16 (2017) 94, https://doi.org/10.1186/s12943-017-0663-2.
[8] J. Salzman, Circular RNA expression: its potential regulation and function, Trends Genet. 32 (2016) 309–316, https://doi.org/10.1016/j.tig.2016.03.002.
[9] A. Rybak-Wolf, C. Stottmeister, P. Glažar, M. Jens, N. Pino, S. Giusti, M. Hanan, M. Behm, O. Bartok, R. Ashwal-Fluss, M. Herzog, L. Schreyer, P. Papavasileiou, A. Ivanov, M. Öhman, D. Refojo, S. Kadener, N. Rajewsky, Circular RNAs in the mammalian brain are highly abundant, conserved, and dynamically expressed, Mol. Cell. 58 (2015) 870–885, https://doi.org/10.1016/j.molcel.2015.03.027.
[10] D. Zhou, L. Dong, L. Yang, Q. Ma, F. Liu, Y. Li, S. Xiong, Identification and analysis of circRNA-miRNA-mRNA regulatory network in hepatocellular carcinoma, IET Syst. Biol. 14 (2020) 391–398, https://doi.org/10.1049/iet-syb.2020.0061.
[11] W.W. Du, C. Zhang, W. Yang, T. Yong, F.M. Awan, B.B. Yang, Identifying and characterizing circRNA-protein interaction, Theranostics 7 (2017) 4183–4191, https://doi.org/10.7150/thno.21299.
[12] P. Wu, Y. Mo, M. Peng, T. Tang, Y. Zhong, X. Deng, F. Xiong, C. Guo, X. Wu, Y. Li, X. Li, G. Li, Z. Zeng, W. Xiong, Emerging role of tumor-related functional peptides encoded by lncRNA and circRNA, Mol. Cancer 19 (2020) 22, https://doi.org/10.1186/s12943-020-1147-3.
[13] X. Zhang, J. Lu, Q. Zhang, Q. Luo, B. Liu, CircRNA RSF1 regulated ox-LDL induced vascular endothelial cells proliferation, apoptosis and inflammation through modulating miR-135b-5p/HDAC1 axis in atherosclerosis, Biol. Res. 54 (2021) 11, https://doi.org/10.1186/s40659-021-00335-5.
[14] Q.S. Peng, Y.N. Cheng, W.B. Zhang, H. Fan, Q.H. Mao, P. Xu, circRNA_0000140 suppresses oral squamous cell carcinoma growth and metastasis by targeting miR-31 to inhibit Hippo signaling pathway, Cell Death Dis. 11 (2020) 112, https://doi.org/10.1038/s41419-020-2273-y.
[15] L. Qin, Z. Zhan, C. Wei, X. Li, T. Zhang, J. Li, Hsa-circRNA-G004213 promotes cisplatin sensitivity by regulating miR-513b-5p/PRPF39 in liver cancer, Mol. Med. Rep. 23 (2021), https://doi.org/10.3892/mmr.2021.12060.
[16] W.C. Liang, C.W. Wong, P.P. Liang, M. Shi, Y. Cao, S.T. Rao, S.K. Tsui, M.M. Waye, Q. Zhang, W.M. Fu, J.F. Zhang, Translation of the circular RNA circβ-catenin promotes liver cancer cell growth through activation of the Wnt pathway, Genome Biol. 20 (2019) 84, https://doi.org/10.1186/s13059-019-1685-4.
[17] S. Lamouille, J. Xu, R. Derynck, Molecular mechanisms of epithelial-mesenchymal transition, Nat. Rev. Mol. Cell Biol. 15 (2014) 178–196, https://doi.org/10.1038/nrm3758.
[18] Y. Zhang, R.A. Weinberg, Epithelial-to-mesenchymal transition in cancer: complexity and opportunities, Front. Med. 12 (2018) 361–373, https://doi.org/10.1007/s11684-018-0656-6.

[19] F. Kong, L. Ma, X. Wang, H. You, K. Zheng, R. Tang, Regulation of epithelial-mesenchymal transition by protein lysine acetylation, Cell Commun. Signal. 20 (2022) 57, https://doi.org/10.1186/s12964-022-00870-y.

[20] G. Zhang, G. Zhang, Upregulation of FoxP4 in HCC promotes migration and invasion through regulation of EMT, Oncol. Lett. 17 (2019) 3944–3951, https://doi.org/10.3892/ol.2019.10049.

[21] X.W. Zhang, S.L. Li, D. Zhang, X.L. Sun, H.J. Zhai, RP11-619L19.2 promotes colon cancer development by regulating the miR-1271-5p/CD164 axis, Oncol. Rep. 44 (2020) 2419–2428, https://doi.org/10.3892/or.2020.7794.

[22] Y. Zhong, Y. Du, X. Yang, Y. Mo, C. Fan, F. Xiong, D. Ren, X. Ye, C. Li, Y. Wang, F. Wei, C. Guo, X. Wu, X. Li, Y. Li, G. Li, Z. Zeng, W. Xiong, Circular RNAs function as ceRNAs to regulate and control human cancer progression, Mol. Cancer 17 (2018) 79, https://doi.org/10.1186/s12943-018-0827-8.

[23] X. Yan, Z. Zhu, S. Xu, L.N. Yang, X.H. Liao, M. Zheng, D. Yang, J. Wang, D. Chen, L. Wang, X. Liu, J. Liu, R.H. Chen, X.Z. Zhou, K.P. Lu, H. Liu, MicroRNA-140-5p inhibits hepatocellular carcinoma by directly targeting the unique isomerase Pin1 to block multiple cancer-driving pathways, Sci. Rep. 7 (2017), 45915, https://doi.org/10.1038/srep45915.

[24] G. He, J. Qiu, C. Liu, B. Tian, D. Cai, S. Liu, MiR-148b-3p regulates the expression of DTYMK to drive hepatocellular carcinoma cell proliferation and metastasis, Front. Oncol. 11 (2021), 625566, https://doi.org/10.3389/fonc.2021.625566.

[25] T. Yin, M.M. Liu, R.T. Jin, J. Kong, S.H. Wang, W.B. Sun, miR-152-3p Modulates hepatic carcinogenesis by targeting cyclin-dependent kinase 8, Pathol. Res. Pract. 215 (2019), 152406, https://doi.org/10.1016/j.prp.2019.03.034.

[26] Y. Chu, M. Jiang, F. Du, D. Chen, T. Ye, B. Xu, X. Li, W. Wang, Z. Qiu, H. Liu, Y. Nie, J. Liang, D. Fan, miR-204-5p suppresses hepatocellular cancer proliferation by regulating homeoprotein SIX1 expression, FEBS. Open. Bio. 8 (2018) 189–200, https://doi.org/10.1002/2211-5463.12363.

[27] G. Jiang, L. Wen, W. Deng, Z. Jian, H. Zheng, Regulatory role of miR-211-5p in hepatocellular carcinoma metastasis by targeting ZEB2, Biomed, Pharmacother 90 (2017) 806–812, https://doi.org/10.1016/j.biopha.2017.03.081.

[28] M. Hanan, A. Simchovitz, N. Yayon, S. Vaknine, R. Cohen-Fultheim, M. Karmon, N. Madrer, T.M. Rohrlich, M. Maman, E.R. Bennett, D.S. Greenberg, E. Meshorer, E.Y. Levanon, H. Soreq, S. Kadener, A Parkinson's disease CircRNAs Resource reveals a link between circSLC8A1 and oxidative stress, EMBO Mol. Med. 12 (2020), e11942, https://doi.org/10.15252/emmm.201911942.

[29] C. Braicu, C. Burz, I. Berindan-Neagoe, O. Balacescu, F. Graur, V. Cristea, A. Irimie, Hepatocellular carcinoma: tumorigenesis and prediction markers, Gastroenterology. Res 2 (2009) 191–199, https://doi.org/10.4021/gr2009.07.1304.

[30] H. Samant, H.S. Amiri, G.B. Zibari, Addressing the worldwide hepatocellular carcinoma: epidemiology, prevention and management, J. Gastrointest. Oncol. 12 (2021) S361–S373, https://doi.org/10.21037/jgo.2020.02.08.

[31] W. Wang, C. Wei, Advances in the early diagnosis of hepatocellular carcinoma, Genes. Dis. 7 (2020) 308–319, https://doi.org/10.1016/j.gendis.2020.01.014.

[32] C. Xue, G. Li, Q. Zheng, X. Gu, Z. Bao, J. Lu, L. Li, The functional roles of the circRNA/Wnt axis in cancer, Mol. Cancer 21 (2022) 108, https://doi.org/10.1186/s12943-022-01582-0.

[33] P. Zheng, H. Gao, X. Xie, P. Lu, Plasma exosomal hsa_circ_0015286 as a potential diagnostic and prognostic biomarker for gastric cancer, Pathol. Oncol. Res. 28 (2022), 1610446, https://doi.org/10.3389/pore.2022.1610446.

[34] X. Jian, H. He, J. Zhu, Q. Zhang, Z. Zheng, X. Liang, L. Chen, M. Yang, K. Peng, Z. Zhang, T. Liu, Y. Ye, H. Jiao, S. Wang, W. Zhou, Y. Ding, T. Li, Hsa_circ_001680 affects the proliferation and migration of CRC and mediates its chemoresistance by regulating BMI1 through miR-340, Mol. Cancer 19 (2020) 20, https://doi.org/10.1186/s12943-020-1134-8.

[35] W. Zhou, F. Yang, Circular RNA circRNA-0039459 promotes the migration, invasion, and proliferation of liver cancer cells through the adsorption of miR-432, Bioengineered 13 (2022) 11810–11821, https://doi.org/10.1080/21655979.2022.2073129.

[36] N. Jia, Z. Song, B. Chen, J. Cheng, W. Zhou, A novel circular RNA circCSPP1 promotes liver cancer progression by sponging miR-1182, OncoTargets Ther. 14 (2021) 2829–2838, https://doi.org/10.2147/OTT.S292320.

[37] Q. Chen, Z. Chen, S. Cao, B. Guo, Y. Chen, Z. Feng, J. Wang, G. Guo, X. Chen, X. Huang, Role of CircRNAs_100395 in proliferation and metastases of liver cancer, Med. Sci. Monit. 25 (2019) 6181–6192, https://doi.org/10.12659/MSM.915963.

[38] L. Wang, Y.F. Shen, Z.M. Shi, X.J. Shang, D.L. Jin, F. Xi, Overexpression miR-211-5p hinders the proliferation, migration, and invasion of thyroid tumor cells by downregulating SOX11, J. Clin. Lab. Anal. 32 (2018), https://doi.org/10.1002/jcla.22293.

[39] M. Li, J. Cai, X. Han, Y. Ren, Downregulation of circNRIP1 suppresses the paclitaxel resistance of ovarian cancer via regulating the miR-211-5p/HOXC8 Axis, Cancer Manag. Res. 12 (2020) 9159–9171, https://doi.org/10.2147/CMAR.S268872.

[40] S. Yi, M. Yu, S. Yang, R.J. Miron, Y. Zhang, Tcf12, A member of basic helix-loop-helix transcription factors, mediates bone marrow mesenchymal stem cell osteogenic differentiation in vitro and in vivo, stem, Cells 35 (2017) 386–397, https://doi.org/10.1002/stem.2491.

[41] J. Yang, L. Zhang, Z. Jiang, C. Ge, F. Zhao, J. Jiang, H. Tian, T. Chen, H. Xie, Y. Cui, M. Yao, H. Li, J. Li, TCF12 promotes the tumorigenesis and metastasis of hepatocellular carcinoma via upregulation of CXCR4 expression, Theranostics 9 (2019) 5810–5827, https://doi.org/10.7150/thno.34973.

[42] Q.B. Chen, Y.K. Liang, Y.Q. Zhang, M.Y. Jiang, Z.D. Han, Y.X. Liang, Y.P. Wan, J. Yin, H.C. He, W.D. Zhong, Decreased expression of TCF12 contributes to progression and predicts biochemical recurrence in patients with prostate cancer, Tumour. Biol. 39 (2017), 1010428317703924, https://doi.org/10.1177/1010428317703924.

[43] J. He, S. Shen, W. Lu, Y. Zhou, Y. Hou, Y. Zhang, Y. Jiang, H. Liu, Y. Shao, HDAC1 promoted migration and invasion binding with TCF12 by promoting EMT progress in gallbladder cancer, Oncotarget 7 (2016) 32754–32764, https://doi.org/10.18632/oncotarget.8740.

[44] C.C. Lee, W.S. Chen, C.C. Chen, L.L. Chen, Y.S. Lin, C.S. Fan, T.S. Huang, TCF12 protein functions as transcriptional repressor of E-cadherin, and its overexpression is correlated with metastasis of colorectal cancer, J. Biol. Chem. 287 (2012) 2798–2809, https://doi.org/10.1074/jbc.M111.258947.

[45] G.D. Marconi, L. Fonticoli, T.S. Rajan, S.D. Pierdomenico, O. Trubiani, J. Pizzicannella, F. Diomede, Epithelial-mesenchymal transition (EMT): the type-2 EMT in wound healing, tissue regeneration and organ fibrosis, Cells 10 (2021), https://doi.org/10.3390/cells10071587.

[46] T.T. Onder, P.B. Gupta, S.A. Mani, J. Yang, E.S. Lander, R.A. Weinberg, Loss of E-cadherin promotes metastasis via multiple downstream transcriptional pathways, Cancer Res. 68 (2008) 3645–3654, https://doi.org/10.1158/0008-5472.CAN-07-2938.

[47] C.L.T. Jørgensen, C. Forsare, P.O. Bendahl, A.K. Falck, M. Fernö, K. Lövgren, K. Aaltonen, L. Rydén, Expression of epithelial-mesenchymal transition-related markers and phenotypes during breast cancer progression, Breast Cancer Res. Treat. 181 (2020) 369–381, https://doi.org/10.1007/s10549-020-05627-0.

[48] R. Shi, W. Zhang, J. Zhang, Z. Yu, L. An, R. Zhao, X. Zhou, Z. Wang, S. Wei, H. Wang, CircESRP1 enhances metastasis and epithelial-mesenchymal transition in endometrial cancer via the miR-874-3p/CPEB4 axis, J. Transl. Med. 20 (2022) 139, https://doi.org/10.1186/s12967-022-03334-6.

[49] G. Zhu, S. Yang, R. Wang, J. Lei, P. Ji, J. Wang, K. Tao, C. Yang, S. Ge, L. Wang, P53/miR-154 pathway regulates the epithelial-mesenchymal transition in glioblastoma multiforme cells by targeting TCF12, neuropsychiatr, Dis. Treat. 17 (2021) 681–693, https://doi.org/10.2147/NDT.S273578.